

Missing Quasiparticles and the Chemical Potential Puzzle in the Doping Evolution of the Cuprate Superconductors

K. M. Shen,¹ F. Ronning,^{1,*} D. H. Lu,¹ W. S. Lee,¹ N. J. C. Ingle,¹ W. Meevasana,¹ F. Baumberger,¹ A. Damascelli,^{1,†} N. P. Armitage,^{1,‡} L. L. Miller,² Y. Kohsaka,³ M. Azuma,⁴ M. Takano,⁴ H. Takagi,³ and Z.-X. Shen¹

¹*Departments of Applied Physics, Physics, and Stanford Synchrotron Radiation Laboratory, Stanford University, Stanford, California 94305, USA*

²*Department of Chemistry, University of Oregon, Eugene, Oregon 97403, USA*

³*Department of Advanced Materials Science, University of Tokyo, Kashiwa, Chiba 277-8561, Japan*

⁴*Institute for Chemical Research, Kyoto University, Uji, Kyoto 611-0011, Japan*

(Received 19 May 2004; published 20 December 2004)

The evolution of $\text{Ca}_{2-x}\text{Na}_x\text{CuO}_2\text{Cl}_2$ from Mott insulator to superconductor was studied using angle-resolved photoemission spectroscopy. By measuring both the excitations near the Fermi energy as well as nonbonding states, we tracked the doping dependence of the electronic structure and the chemical potential with unprecedented precision. Our work reveals failures in the standard weakly interacting quasiparticle scenario, including the broad line shapes of the insulator and the apparently paradoxical shift of the chemical potential within the Mott gap. To resolve this, we develop a model where the quasiparticle is vanishingly small at half filling and grows upon doping, allowing us to unify properties such as the dispersion and Fermi wave vector with the chemical potential.

DOI: 10.1103/PhysRevLett.93.267002

PACS numbers: 74.25.Jb, 74.72.Jt, 79.60.-i

A central intellectual issue in the field of high-temperature superconductivity is how an antiferromagnetic insulator evolves into a superconductor. In principle, the ideal tool to address this problem is angle-resolved photoemission spectroscopy (ARPES), which can directly extract the single-particle excitations. Despite the great interest in this subject, there continues to be a lack of consensus, perhaps the most prominent example being the controversy over the chemical potential, μ . Over the past 15 years, there have been conflicting claims of μ either being pinned in midgap or shifting to the valence or conduction band upon carrier doping [1–6]. The inability of photoemission spectroscopy to provide a logically consistent understanding of this fundamental thermodynamic quantity has been a dramatic shortcoming in the field.

In this Letter, we present a new procedure to quantify μ precisely while permitting simultaneous high resolution ARPES measurements on the low-energy states. This approach has allowed us to make major conceptual advances in addressing the doping evolution. We find that the long standing confusion over μ stems from the manner in which quasiparticlelike (QP) excitations in the doped samples emerge from the unusually broad peak in the undoped insulator, which was previously and mistakenly believed to represent the QP pole. On the one hand, we find that μ changes in a manner consistent with an approximate rigid band shift; on the other hand, this shift appears to occur *within* the apparent Mott (or charge-transfer) gap of the parent insulator. We show that this ostensible paradox can be naturally resolved if one uses a model based on Franck-Condon broadening (FCB) where the QP residue, Z , is vanishingly small near half filling.

This reconciles existing puzzles regarding the insulator and the lightly doped compounds, and naturally ties the behavior of μ to low-energy features such as the Fermi wave vector, \mathbf{k}_F , and the QP velocity v_F .

$\text{Ca}_{2-x}\text{Na}_x\text{CuO}_2\text{Cl}_2$ is an ideal system to address the doping evolution of the cuprates. The stoichiometric parent compound, $\text{Ca}_2\text{CuO}_2\text{Cl}_2$, is chemically stable and, along with its close variants, has served as the prototype for the undoped Mott insulator [1,7]. The system possesses a simple structure, with a single CuO_2 layer devoid of known superlattice modulations, structural distortions, or surface states. The $x = 0.10$ and 0.12 samples had T_c 's of 13 and 22 K, respectively ($T_{c,\text{opt}} = 28$ K), while the $x = 0.05$ composition was nonsuperconducting, and were grown using a high pressure flux method [8]. ARPES measurements were performed at Beamline 5-4 of the Stanford Synchrotron Radiation Laboratory with typical energy and angular resolutions of 13 meV and 0.3° , respectively, using photon energies of 21.2 and 25.5 eV. Measurements were performed at 15 K, except for $x = 0$, which was measured at $T > 180$ K.

Previous quantitative studies of μ have relied on core level spectroscopy which can be difficult to interpret. Since measuring μ is of paramount importance, we introduce a new approach which we believe to be more accurate and direct. Our method uses orbitals in the valence band which are completely occupied but reside at low energies (< 5 eV). We treat these as delocalized bandlike states, an assumption supported by their agreement with band structure. Therefore, their shift with doping should simply represent the change in μ . We believe this simple “rigid band” model is justified by the fact that the general shape of the valence band re-

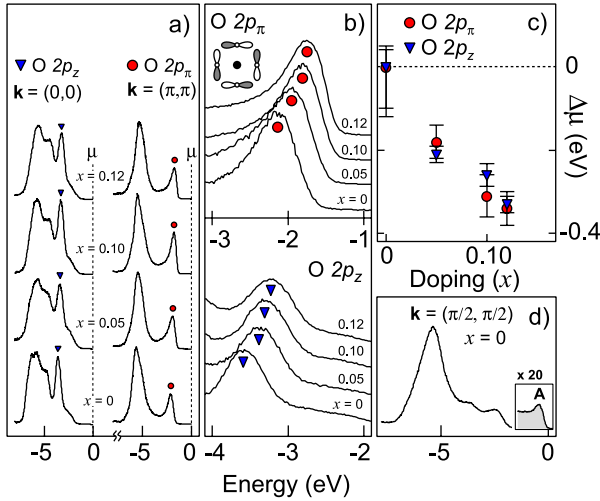


FIG. 1 (color online). (a) Valence band spectra for $x = 0, 0.05, 0.10,$ and 0.12 compositions at $\mathbf{k} = (0, 0)$ and (π, π) . $O 2p_z$ and $O 2p_\pi$ states are marked by triangles and circles, respectively. (b) Shifts of the $O 2p_z$ and $O 2p_\pi$ peaks shown on an expanded scale. (c) Doping dependence of μ determined from (b). (d) Valence band at $\mathbf{k} = (\pi/2, \pi/2)$, showing the lower Hubbard band (A) on an expanded scale.

mains qualitatively unchanged with doping, apart from this shift [Fig. 1(a)].

In particular, we have selected $O 2p$ states [$O 2p_z$ at $(0, 0)$ and $O 2p_\pi$ at (π, π)] which are nonbonding with the Cu $3d_{x^2-y^2}$ orbital or Zhang-Rice singlet [9,10]. The $O 2p_z$ orbital is directed out of the CuO_2 plane. The $O 2p_\pi$ band is arranged in an in-plane, antibonding configuration shown in Fig. 1(b) at (π, π) , with an estimated separation of ~ 3 eV from the bonding configuration at $\mathbf{k} = (\pi, \pi)$ [11], although hybridization of the bonding band with the Cu $3d_{xy}$ orbital modifies this value by up to ~ 2 eV [10]. In Fig. 1(b), we show the shift of the $O 2p_z$ and $O 2p_\pi$ peaks on an expanded scale plotted relative to chemical potential, demonstrating the change in μ . This data is summarized in Fig. 1(c), with statistics collected from >5 samples for each concentration and referenced to the $x = 0$ composition; we describe the methodology for determining μ_0 later in the text. The shift from these marker states yields $\mu_{0.05} = -0.20$ eV, $\mu_{0.10} = -0.28$ eV, and $\mu_{0.12} = -0.33$ eV, all relative to μ_0 , with a typical uncertainty of ± 0.025 eV. At finite x , $(\partial\mu/\partial x) = -1.8 \pm 0.5$ eV/hole, comparable to estimates from band structure (~ -1.3 eV/hole) [12].

We now turn our attention from the higher energy $O 2p$ bands to the lowest lying state, the $O 2p$ and Cu $3d_{x^2-y^2}$ derived lower Hubbard band (or more precisely, charge-transfer band) denoted as A in Fig. 1(d). The above measurements of μ have revealed a fundamental failure of the traditional framework where this main peak of the lower Hubbard band in the insulator represents a QP, along the lines of the weakly interacting, Fermi liquid-

like picture, which we call the “coherent quasiparticle scenario” (CQS). In the CQS, all energies above the peak maximum should fall within the Mott gap. As shown in Fig. 1, μ shifts by an amount compatible with predictions from band structure calculations. However, this shift appears to occur *within the apparent Mott gap*—a logical inconsistency as there are no available states within the gap to shift into [Fig. 2(a), left]. While impuritylike states may form within the gap, in this picture μ should not drop so rapidly with doping. By combining measurements of both μ and the near- E_F states, our new results suggest an alternative picture inspired by FCB [Fig. 2(a), right].

To understand the failings of the CQS, the obvious starting point is the parent insulator. Early studies of $\text{Ca}_2\text{CuO}_2\text{Cl}_2$ and $\text{Sr}_2\text{CuO}_2\text{Cl}_2$ yielded broad peaks with a dispersion consistent with calculations from the extended t - J model [1,7,13], and were interpreted as QP poles. However, one crucial point that remained unresolved was the extreme width of these excitations. We address this as a critical flaw of the CQS, and use this as a starting point for constructing a new model. Data taken at the top of the lower Hubbard band, $\mathbf{k} = (\pi/2, \pi/2)$, are shown in Fig. 2 where one should expect the peak width, Γ , to be extremely narrow due to electron scattering phase space constraints. Instead, Γ is comparable to the entire bandwidth $2J \sim 350$ meV, completely inconsistent with such a picture. Moreover, the width

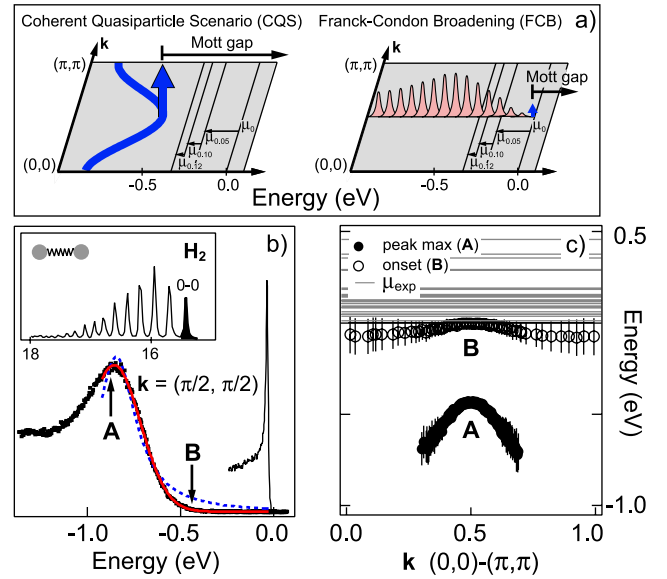


FIG. 2 (color online). (a) Illustrations of the coherent quasiparticle scenario (CQS) and the Franck-Condon broadening (FCB) model. (b) $\text{Ca}_2\text{CuO}_2\text{Cl}_2$ at $\mathbf{k} = (\pi/2, \pi/2)$ with fits to a Lorentzian spectral function (dashed) and Gaussian (red or gray). A and B denote the peak maximum and the onset of spectral weight, respectively. Comparison with Sr_2RuO_4 is shown (thin black). Upper inset shows photoemission spectra from H_2 , after Ref. [26]. (c) Dispersion of A and B along $(0, 0) - (\pi, \pi)$, along with experimental values for μ (lines).

cannot be due to disorder, as the undoped system is stoichiometric, and adding chemical dopants results in sharper structures, as will be shown. For comparison, we also present spectra from Sr_2RuO_4 (thin black) exhibiting a nearly resolution-limited peak. Given that well-defined QP excitations can be observed by ARPES, we must confront the origin of the broad peaks in $\text{Ca}_2\text{CuO}_2\text{Cl}_2$. Moreover, in the CQS, the peak in Fig. 2(b) should be well described by a spectral function $\mathcal{A}(\mathbf{k}, \omega) = -(1/\pi) \times \{\Sigma''/[(\omega - \epsilon_{\mathbf{k}} - \Sigma')^2 + (\Sigma'')^2]\}$, which should be approximately Lorentzian with a width dominated by an impurity scattering term, Γ_{imp} [1]. A fit of $\mathcal{A}(\mathbf{k}, \omega)$ to the experimental data is shown and agrees poorly, even when assuming an unphysically large Γ_{imp} (~ 300 meV), given that the material is stoichiometric.

In light of this failure of the CQS, we believe that an analogy to one of the simplest quantum systems, the H_2 molecule, may be enlightening. The $\text{H}_2 \rightarrow \text{H}_2^+$ photoemission spectrum, shown in the upper inset of Fig. 2(b), exhibits FCB. Only the “0-0” peak (filled black) represents the H_2^+ final state with no excited vibrations and comprises only $\sim 10\%$ of the intensity. In the solid state, 0-0 alone would represent the QP or the coherent part of the spectral function, \mathcal{A}_{coh} , whereas the excited states comprise the incoherent part, \mathcal{A}_{inc} . This behavior is redolent of polarons, and such models have been suggested in systems where strong couplings are present [14–16]. The low-energy tail is suppressed exponentially, inconsistent with power law falloffs from $\mathcal{A}(\mathbf{k}, \omega)$ line shapes, but well described by FCB predictions of a Gaussian envelope.

Another unresolved issue is a large energy scale separating the peak from the experimental positions of μ . For an insulator, μ is not well defined, and is pinned by surface defects and impurities and will vary between samples. However, the limits of this distribution are well defined, with a lower bound set by the QP pole at the top of the valence band. For this study, we identify two features: the peak maximum (A), and the onset of intensity (B), determined by a 3σ signal above background. In Fig. 2(c), we show the dispersion of A and B along $(0,0)$ - (π, π) . While A qualitatively tracks the dispersion of the t - J model, B disperses only weakly and has a separation of ~ 450 meV from A. We present the distribution of μ_{exp} from numerous samples in Fig. 2(c) and B clearly sets a lower bound for the distribution of μ_{exp} . This behavior suggests that the true QP (B) is hidden within the tail of spectral intensity, and A is simply incoherent weight associated with shake-off excitations. For $x = 0$, we reference A and the valence band features such that B is aligned to 0. This demarcates the upper bound for both the QP at half filling and $\mu(x = 0^+)$, which take as μ_0 . This model is also consistent with the temperature dependence of the line shape, where a similar multiple initial/final state model was proposed [17].

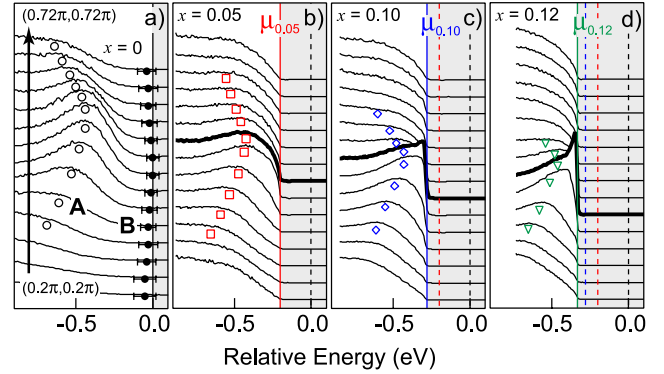


FIG. 3 (color online). (a)–(d) EDC spectra from $x = 0, 0.05, 0.10,$ and 0.12 from $(0.2\pi, 0.2\pi)$ to $(0.72\pi, 0.72\pi)$ with hump positions marked by open symbols and \mathbf{k}_F shown in bold. Data are plotted on a relative energy scale referenced to the shift in μ shown in Fig. 1(c).

There are a number of possible mechanisms for this line shape broadening. Although some approximate analytical calculations have predicted that interactions with the spin background cause $Z \rightarrow 0$ [18,19], the majority of exact numerical simulations of the pure t - J model show that Z remains finite ($Z \sim 0.2$) [20]. Therefore we believe lattice effects are a likely candidate, and our data bears some resemblance to lattice polaronic systems [14–16]. Recent calculations incorporating lattice effects into the t - J model have reproduced the most salient features of the ARPES spectra, including a vanishing QP peak (B) and a broad hump (A) which recovers the original t - J dispersion [21]. However, more work is necessary before the origin of the FCB can be conclusively determined.

In Fig. 3, we show the doping evolution of the near- E_F energy distribution curves (EDCs), from $(0.2\pi, 0.2\pi)$ to $(0.72\pi, 0.72\pi)$. All data are plotted relative to μ_0 using the values determined in Fig. 1(c). With doping, feature A evolves smoothly into a broad, high energy hump with a backfolded dispersion similar to the parent insulator (symbols), while μ shifts downward from B. It is now clear that μ does not fall immediately to A upon hole doping as expected in the CQS. Spectral weight develops at μ , and a well-defined peak becomes visible for the $x = 0.10$ and 0.12 compositions, comprising a coherent, low-energy band. The dispersion of the hump (A) is summarized in Fig. 4(a), and was determined by tracking the local maxima or second derivatives of the EDCs, but does not represent any precise physical quantity. Feature A remains fixed at high energies with doping, justifying our model which decouples A from μ .

We also track the dispersion of the lowest energy excitations (-0.05 eV $< \omega < E_F$) from a momentum distribution curve (MDC) analysis (lines). The dispersion of the low-energy states reveals a remarkable universal behavior across doping levels where both the velocities of the QP dispersion (v_F) and Fermi wave vectors (\mathbf{k}_F) virtually collapse onto a single straight line, with a

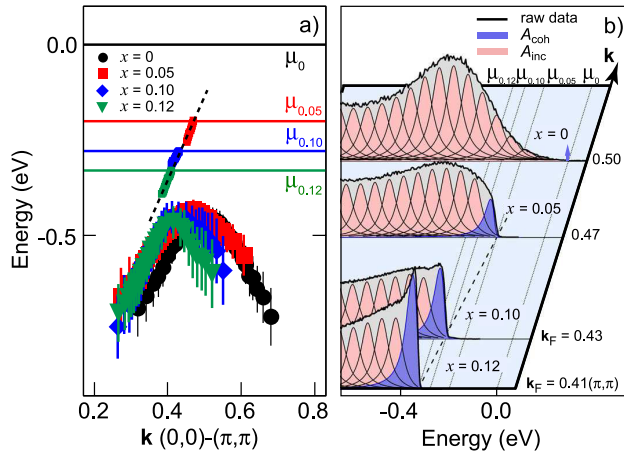


FIG. 4 (color online). (a) Summary of hump (symbols) and MDC dispersions (lines) from Fig. 3. (b) Doping dependence of spectra from \mathbf{k}_F along with a schematic of the proposed distribution of coherent (blue or dark gray) and incoherent (pink or light gray) spectral weight.

band velocity (1.8 eV \AA) corresponding closely to the recently discovered “universal nodal velocity” [22]. This result also ties μ to the QP dispersion to explain how \mathbf{k}_F evolves with doping, with $\Delta \mathbf{k}_F \sim \Delta \mu / v_F$. We note that a number of different theoretical proposals have predicted the emergence of sharp QP-like excitations from broad features, including dynamical mean-field theories [23] or “gossamer” superconductivity [24]. Figure 4(b) is a schematic summary of the doping-induced transfer between coherent (blue or dark gray) and incoherent (pink or light gray) spectral weight. This explains the apparent absence of a peak for $x = 0.05$, as it is overwhelmed by the incoherent weight, and also demonstrates that neither in-gap states nor a rigid band shift were adequate models in the FCB context. A similar QP emergence was also observed in $\text{La}_{2-x}\text{Sr}_x\text{CuO}_4$ [25], although with a larger separation between A and E_F [1].

In conclusion, we have developed a phenomenological model based on high precision measurements of μ and detailed studies of the near- E_F states, providing us with the first globally consistent understanding of the doping evolution of the cuprates. This picture can be summarized as follows. (i) At half filling, Z is vanishingly small, reminiscent of FCB. The true QP is found in the long tail of spectral intensity. (ii) The misidentification of the broad peak as the QP pole was at the root of the long standing confusion over μ . (iii) With doping, spectral weight is transferred to the low-energy QP peak. (iv) The shift of the chemical potential and \mathbf{k}_F is dictated by the band velocity of this faint QP band. We believe that this model provides a foundation for the origin of the quasiparticles upon doping and should be used as

a guide to develop microscopic theories for high- T_c superconductivity.

We would like to thank A. Fujimori, C. Kim, and N. Nagaosa for enlightening discussions. SSRL is operated by the DOE Office of Basic Energy Science under Contract No. DE-AC03-765F00515. K. M. S. acknowledges SGF and NSERC for their support. The ARPES measurements at Stanford were also supported by NSF DMR-0304981 and ONR N00014-98-1-0195.

*Present address: Los Alamos National Laboratory, Los Alamos, NM 87545, USA.

†Present address: Department of Physics and Astronomy, University of British Columbia, Vancouver, B.C., Canada, V6T 1Z1.

‡Present address: Department of Physics and Astronomy, University of CA, Los Angeles, Los Angeles, CA 90095, USA.

- [1] A. Damascelli, Z. Hussain, and Z.-X. Shen, *Rev. Mod. Phys.* **75**, 473 (2003).
- [2] J.W. Allen *et al.*, *Phys. Rev. Lett.* **64**, 595 (1990).
- [3] Z.-X. Shen *et al.*, *Phys. Rev. B* **44**, 12098 (1991).
- [4] A. Ino *et al.*, *Phys. Rev. Lett.* **79**, 2101 (1997).
- [5] P.G. Steeneken *et al.*, *Phys. Rev. Lett.* **90**, 247005 (2003).
- [6] F. Ronning *et al.*, *Phys. Rev. B* **67**, 165101 (2003).
- [7] B.O. Wells *et al.*, *Phys. Rev. Lett.* **74**, 964 (1995).
- [8] Y. Kohsaka *et al.*, *J. Am. Chem. Soc.* **124**, 12275 (2002).
- [9] J.J.M. Pothuisen *et al.*, *Phys. Rev. Lett.* **78**, 717 (1997).
- [10] R. Hayn *et al.*, *Phys. Rev. B* **60**, 645 (1999).
- [11] L. F. Mattheiss and D. R. Hamann, *Phys. Rev. B* **40**, 2217 (1989).
- [12] L. F. Mattheiss, *Phys. Rev. B* **42**, 354 (1990).
- [13] T. Tohyama and S. Maekawa, *Supercond. Sci. Technol.* **13**, R17 (2000)
- [14] L. Perfetti *et al.*, *Phys. Rev. B* **66**, 075107 (2002).
- [15] D.S. Dessau *et al.*, *Phys. Rev. Lett.* **81**, 192 (1998).
- [16] V. Perebeinos and P.B. Allen, *Phys. Rev. Lett.* **85**, 5178 (2000).
- [17] C. Kim *et al.*, *Phys. Rev. B* **65**, 174516 (2002).
- [18] B. I. Shraiman, and E. D. Siggia, *Phys. Rev. Lett.* **61**, 467 (1988).
- [19] D. N. Sheng, Y. C. Chen, and Z. Y. Weng, *Phys. Rev. Lett.* **77**, 5102 (1996).
- [20] E. Dagotto, *Rev. Mod. Phys.* **66**, 763 (1994).
- [21] A. S. Mishchenko and N. Nagaosa, *Phys. Rev. Lett.* **93**, 036402 (2004).
- [22] X. J. Zhou *et al.*, *Nature (London)* **423**, 398 (2003).
- [23] A. Georges *et al.*, *Rev. Mod. Phys.* **68**, 13 (1996).
- [24] B. A. Bernevig, R. B. Laughlin, and D. I. Santiago, *Phys. Rev. Lett.* **91**, 147003 (2003).
- [25] T. Yoshida *et al.*, *Phys. Rev. Lett.* **91**, 027001 (2003).
- [26] D.W. Turner, *Molecular Photoelectron Spectroscopy* (Wiley, New York, 1970).